

Microflower like Zinc Oxide/Cerium, Lanthanum Substituted Hydroxyapatite Bilayer Coating on Surgical Grade Stainless Steel for Corrosion Resistance, Antibacterial and Bioactive Properties

C. SRIDEVI¹, P. KARTHIKEYAN², D. DHIVYAPRIYA¹, L. MITU³, P. MAHESWARAN¹ and S. SATHISHKUMAR^{4,*}

¹Department of Chemistry, P.G.P. College of Arts and Science, Namakkal-637207, India

²Department of Chemistry, Periyar University Constituent College of Arts and Science, Idappadi, Salem-637102, India

³Department of Physics & Chemistry, University of Pitesti, Pitesti 110040, Romania

⁴Department of Chemistry, Sri Vijay Vidyalaya College of Arts and Science, Dharmapuri-636807, India

*Corresponding author: E-mail: sathish.sskg@gmail.com

Received: 28 August 2019;

Accepted: 18 November 2019;

Published online: 25 February 2020;

AJC-19797

The growing evidence of beneficial role of zinc in bone has increased the interest of developing zinc-containing biomaterials for medical applications and specifically biocompatible coatings that can be deposited on metallic implants to benefit from their load-bearing capabilities. In present work, zinc oxide/cerium, lanthanum substituted (ZnO/Ce,La-HAP) hydroxyapatite bilayer coatings have been fabricated by electrodeposition technique. As developed, ZnO/Ce,La-HAP bilayer coatings were then structurally, morphologically and chemically characterized using Fourier-transform infrared spectroscopy (FT-IR), X-ray diffraction (XRD), higher resolution scanning electron microscopy (HRSEM) and energy dispersive X-ray spectroscopy (EDAX). The properties of corrosion performance of 316L SS were explored in Ringers solution using electrochemical analysis. The potentiodynamic polarization and impedance analysis demonstrated that the anticorrosion behavior of 316L SS was significantly increased by the bilayer coating. Cell viability *in vitro*, antibacterial activity and live/dead assay of ZnO/Ce,La-HAP bilayer coating were investigated. Hence, development of ZnO/Ce,La-HAP bilayer coating on 316L SS to make it suitable for biomedical applications.

Keywords: Lanthanum, Hydroxyapatite, Bilayer coating, Anti-corrosion, Antibacterial activity.

INTRODUCTION

Biomedical implants have received much interest and intensive research during last few decades as they are used as replacement material of various body parts or organs [1]. For this purpose metallic material which combines good mechanical characteristics, low cost, high corrosion resistance and good compatibility with any of the biological materials, need to be chosen [2]. In order to ensure their long term clinical application and to enhance the bioactivity of 316L SS implants, a bioceramic material with osteoconductive property is often coated on the metallic implants. However, the formation of chromium oxide layer on 316L SS surface tolerate the biological atmosphere and hereafter discharge of metallic ions such as iron, chromium and nickel are evidenced in the human body [3-8]. Therefore, a decrease in Fe, Cr, and Ni ions released and in order to improve the corrosion resistance, osteointe-

gration, and osteocompatibility properties of additional to the biomaterials such as calcium phosphate bioceramics [9,10].

Among the materials used for coating, hydroxyapatite [HAP, Ca₁₀(PO₄)₆(OH)₂] is the best biocompatible and bioactive material that acts as a bridge between implant and human tissue thereby improving the osseointegration [11-15]. HAP in bone is a multi-substituted calcium phosphate, including traces of Mg²⁺, Sr²⁺, Si⁴⁺, CO²⁻, Ba²⁺, Zn²⁺, F⁻, etc. [16,17]. Hence, ionic substitutions in synthetic HAP play an important role in bone formation. There are also several studies on the synthesis and coating of the metal ion substituted HAP which has been shown to improve its structural stability and cellular biocompatible properties. Hence, incorporations of rare earth ions such as La, Ce, Sm, Eu, Gd and Tb in HAP have been the subject of great interest due to the significant role of these ions in the biological process after implantations [18-20]. Lanthanide ions specifically, cerium ion play a significant role as antibacterial

agent in various biomedical fields for achieved. Numerous *in vitro* analysis have been reported the cerium ions in major role in minimizing bacterial adhesion [21,22]. To decrease the toxic nature, secondary material having good bioactivity can be introduced. The incorporation of lanthanum ions in hydroxyapatite developed the biological and physico-chemical properties of hydroxyapatite.

Tanaka *et al.* [23] and Webster *et al.* [24] reported that lanthanum substituted hydroxyapatite exhibited a superb formation of fibrous tissue around the disc implanted use in bones of rates. In last few decades, various surface modification methods have been established for corrosion protection and enhanced biological properties in 316L SS. One of these techniques is to form a composite by adding reinforcing materials like ZnO, Al₂O₃, ZrO into the HAP. Since, reinforcing material that fulfils all the necessary requirements for biomedical applications, good mechanical property and superior bioactivity. Zinc oxide coating has attracted number of attention for its good corrosion resistance properties and probable applications [25,26]. There are few reports of ZnO coating on 316L SS, which may be promising for the improvement of corrosion resistance and bioactivity of the 316L SS. The objective of present work involves the development of ZnO/Ce,La-HAP bilayer coating on 316L SS. To the best of our knowledge, an improved corrosion and biological properties of ZnO/Ce,La-HAP bilayer coating on the 316LSS implant have not yet been studied. Hence, in this work, ZnO/Ce,La-HAP bilayer coatings for enhancing the corrosion resistance and biocompatibility of 316LSS implant have been fabricated by electrodeposition technique.

EXPERIMENTAL

All the chemicals were analytic grade reagents (purchased from sigma aldrich) and used without further purification.

Preparation of 316L SS specimen: The 316L SS implants obtained from Steel Authority of India, Ltd. (SAIL), India, having an elemental composition (wt. %) of 0.0222 C, 0.551 Si, 1.67 Mn, 0.023 P, 0.0045 S, 17.05 Cr, 11.65 Ni, 2.53 Mo, 0.136 Co, 0.231 Cu, 0.0052 Ti, 0.0783 V, 0.0659 N and Fe (balance), was used as the metal substrate for the electrodeposition. The 316L SS specimens with a size of 10 mm × 10 mm × 3 mm were embedded in epoxy resin, leaving an area of 1 cm² for exposure to the electrolyte solution. Before to electrodeposition, these specimens were abraded with different grades of silicon carbide papers from 400 to 1200 grit. After polishing, these specimens were ultrasonically cleaned and exhaustively washed with acetone and deionized water for 10 min and finally, rinsed in deionized water and dried. In order to enhance the bio-resistivity of 316L SS surface was passivated using 0.4 M borate buffer solution (pH 9.3) at 640 mV *versus* saturated calomel electrode (SCE) for 2 h in potentiostatic condition [27] using electrochemical workstation (Model CHI 760C, CH Instruments, USA).

Preparation of electrolyte solutions

Batch 1: For the preparation of electrolyte solution for ZnO coating, an analytical grade 0.05 M Zn(NO₃)₂·6H₂O was dissolved into 50 mL of ethanol using in solvent an airtight container and stirred continuously for 30 min at room temperature (28 ± 1°C). Then the solution used as precursor.

Batch 2: The electrolyte solution was prepared by dissolving analytical grade 0.3 M Ca(NO₃)₂·6H₂O, 0.1 M La(NO₃)₂·6H₂O and 0.1 M Ce(NO₃)₂·6H₂O in deionized water. Then (NH₄)₂HPO₄ solution (0.3 M) was dissolved in deionized water and the solution was mixed with (La + Ce + Ca)/P molar ratio of 1.67 at room temperature (28 ± 1°C). Then the solution was under magnetic stirring for 4 h and the pH of electrolyte was adjusted to 4.7 using NH₄OH solution.

Development of ZnO coating on 316L SS: The ZnO coating route on 316L SS was carried out in the regular three electrode cell arrangement by galvanostatically technique apply on electrochemical workstation (CHI 760C, CH Instruments, USA) in which 316L SS as the working electrode, platinum electrode served as a counter electrode and saturated calomel electrode (SCE) as the reference electrode for 50 min at various concentration of 0.05, 0.1 and 0.2 M. After electrodeposition, ZnO coating substrates were gently rinsed with deionized water dried in air for 24 h.

Deposition of Ce,La-HAP on ZnO coated 316L SS: In present study, Ce,La-HAP deposition on ZnO coated (0.1M) 316L SS was carried out at constant current density 9 mA/cm² for 35 min. After electrodeposition, ZnO/Ce,La-HAP coating substrates were gently rinsed with deionized water, dried in the air and then stored in a desiccator for further investigations.

Surface characterization of ZnO/Ce,La-HAP coating: The functional groups in ZnO/Ce,La-HAP coating materials were investigated by Fourier transform infrared (FT-IR) spectroscopy. The FT-IR spectra were recorded from 4000-400 cm⁻¹ by using KBr pellet technique. The phase composition of coated samples was studied by X-ray diffraction PANalytical X'Pert PRO diffractometer in the 2θ angle between 200-60° with Cu Kα radiation (1.5406 Å). The surface morphology and actual composition of as a developed ZnO/Ce,La-HAP coating were estimated by a high resolution scanning electron microscopy (HRSEM, JSM 840A, JEOL-Japan) equipped with EDAX.

Electrochemical assessment of ZnO/Ce,La-HAP coating: In this evaluation, potentiodynamic polarization and electrochemical impedance spectroscopy (EIS) of ZnO/Ce,La-HAP coatings on 316L SS specimens in Ringer's solution (NaCl, 8.6 g L⁻¹; CaCl₂·2H₂O, 0.66 g L⁻¹; and KCl, 0.6 g L⁻¹) at pH 7 and at 37 ± 1 °C. The electrochemical investigations were performed in the CHI Model 760 electrochemical workstation (USA) by using three necked cells. The potential values are reported, with respect to SCE. While in the cyclic polarization studies, the potential was raised to the positive shift with a sweep rate of 0.1 mV s⁻¹ until the breakdown potential (E_b) was reached. The sweep direction was reversed until the scan met the positive shift. The breakdown was got at the potential where there was a monotonic increase in the current density. The re-passivation potential (E_{pp}) is the potential at which the reverse scan meets the passive region. The EIS experiments were performed in the same setup as that of potentiodynamic cyclic polarization studies and the applied AC perturbation amplitude was 5 mV within the frequency range from 10⁻² Hz to 100 kHz. The present electrochemical value was engaged using internally available software and the reproducibility of each electrochemical investigation was repeating at least three times.

Antibacterial activity: The *in vitro* antibacterial activity of ZnO/Ce,La-HAP coating at different concentrations have been investigated against two prokaryotic strains such as *S. aureus* (ATCC 25923) and *E. coli* (ATCC 25922) through agar disc diffusion method. The Mullar-Hinton agar plates were prepared by pouring 15 mL of a molten medium into sterile Petri plates. The plates were allowed to solidify for ~15 min and 0.1 % of inoculum suspension was swabbed uniformly over the agar until the inoculums became invisible. Different concentrations (25, 50, 75, 100 and 125 μL) of ZnO/Ce,La-HAP coating were loaded onto 5 mm sterile individual discs, followed by incubation of plates at 37 °C for 24 h. The zone of inhibition was observed by measuring the width of inhibited zone.

Osteocompatibility analysis: The cell proliferation of MC3T3-E1 cells on ZnO/Ce,La-HAP was studied using MTT assay on day 1, 3, 5 and 7 days. To determine the cytotoxicity of the samples at different conditions, MC3T3-E1 cells were seeded in 12-well plates at 10^4 cells/mL in a humidified 5 % CO_2 atmosphere. Each time, 400 μL of MTT reagent (1 mg/mL) was added to each well and incubated for 4 h under the same conditions. Finally, MTT reagent was removed and 400 μL of dimethyl sulfoxide was added for dissolving the formazan crystals and the absorbance was measured at 560 nm in an ELISA microplate reader and then the cell viability (as a percentage) was calculated, with respect to the control as follows:

$$\text{Cell viability (\%)} = \frac{A_{\text{test}}}{A_{\text{control}}} \times 100$$

Live/dead staining: After each culture, cells on ZnO/Ce,La-HAP coated specimens were stained using live/dead assay kit, containing calcein AM and ethidium homodimer. Every time, media discarded and the samples were washed with PBS, then live/dead solution containing 2 mM calcein AM and 4mM ethidium homodimer was added to each well incubated at 37 °C for 20 min. The stained cultures were viewed using a fluorescent (Nikon Eclipse 80i) microscope [28].

Statistical analysis: All the investigations were performed for ZnO/ Ce, La-HAP coating in triplicate and repeated three times (mean \pm SD). Statistical analysis was performed using analysis of variance (ANOVA) with Tukey's multiple comparison tests (Prism, version 5.0). The difference observed between samples was considered to be significant at $P < 0.05$.

RESULTS AND DISCUSSION

FT-IR analysis: Fig. 1 illustrates the FT-IR spectra of ZnO/Ce,La-HAP coating on 316L SS. The stretching and bending vibrational modes of water molecule group were presented at 3570.77 and 1459.82 cm^{-1} , respectively. The characteristic adsorption bands identified at 473.78, 569.75 and 603.14 (ν_4), 961.93 (ν_1), 1026.85 and 1091.62 cm^{-1} (ν_3) correspond to the phosphate group, which were assigned to P-O bending, symmetric P-O stretching vibrations and asymmetric stretching vibrations, respectively. Moreover, the stretching and bending vibrational modes of hydroxyl bands of observed at around 3568.24 and 634.38 cm^{-1} . Thus all the bands confirmed the formation of ZnO/Ce,La-HAP coating on 316L SS and no other impurities were detected.

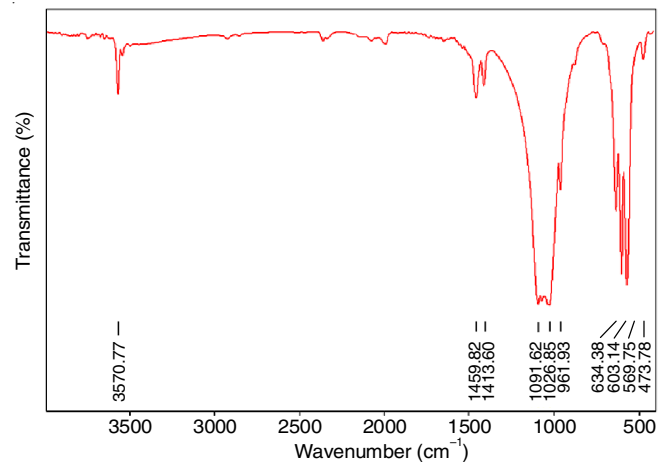


Fig. 1. FT-IR spectra of ZnO/Ce,La-HAP coating on 316L SS

X-ray diffraction analysis: Fig. 2a represents the XRD patterns of ZnO/Ce,La-HAP coating on 316L SS. The broad and intense diffraction peaks are detected at 2θ values of 31.8°, 34.4°, 36.4°, 47.5° and 56.8° for ZnO coated at 316L SS, which were in agreement with International Centre for Diffraction Data (ICDD card no.89-0511). Fig. 2b displays the XRD patterns obtained for ZnO/Ce,La-HAP coating on 316L SS. The main peaks observed at 2θ values of 25.8°, 31.5°, 32.2°, 32.9°, 34.6°, 39.8°, 46.7°, 49.4° and 53.3° corresponds to ZnO/Ce,La-HAP and no other peaks were detected. From these XRD patterns indicate that ZnO/Ce,La-HAP coating were in high crystalline nature and purity.

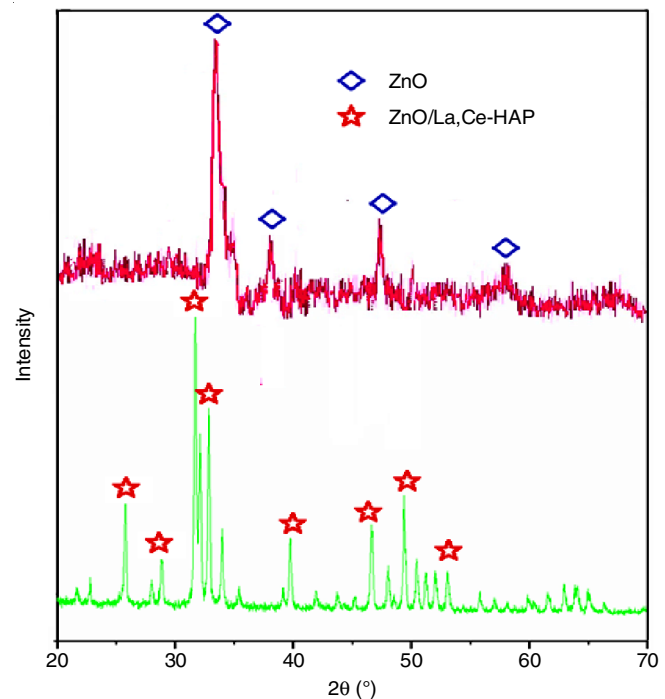


Fig. 2. XRD spectra of (a) ZnO (b) ZnO/Ce,La-HAP coating on 316L SS

Scanning electron microscopic and elemental analysis: Fig. 3 showed the HRSEM images of ZnO, Ce, La-HAP and ZnO/Ce,La-HAP bilayer coating on 316L SS. The surface images ZnO coating on 316L SS deposited at three different concentrations (0.05, 0.1 and 0.2 M) for a duration of 50 min

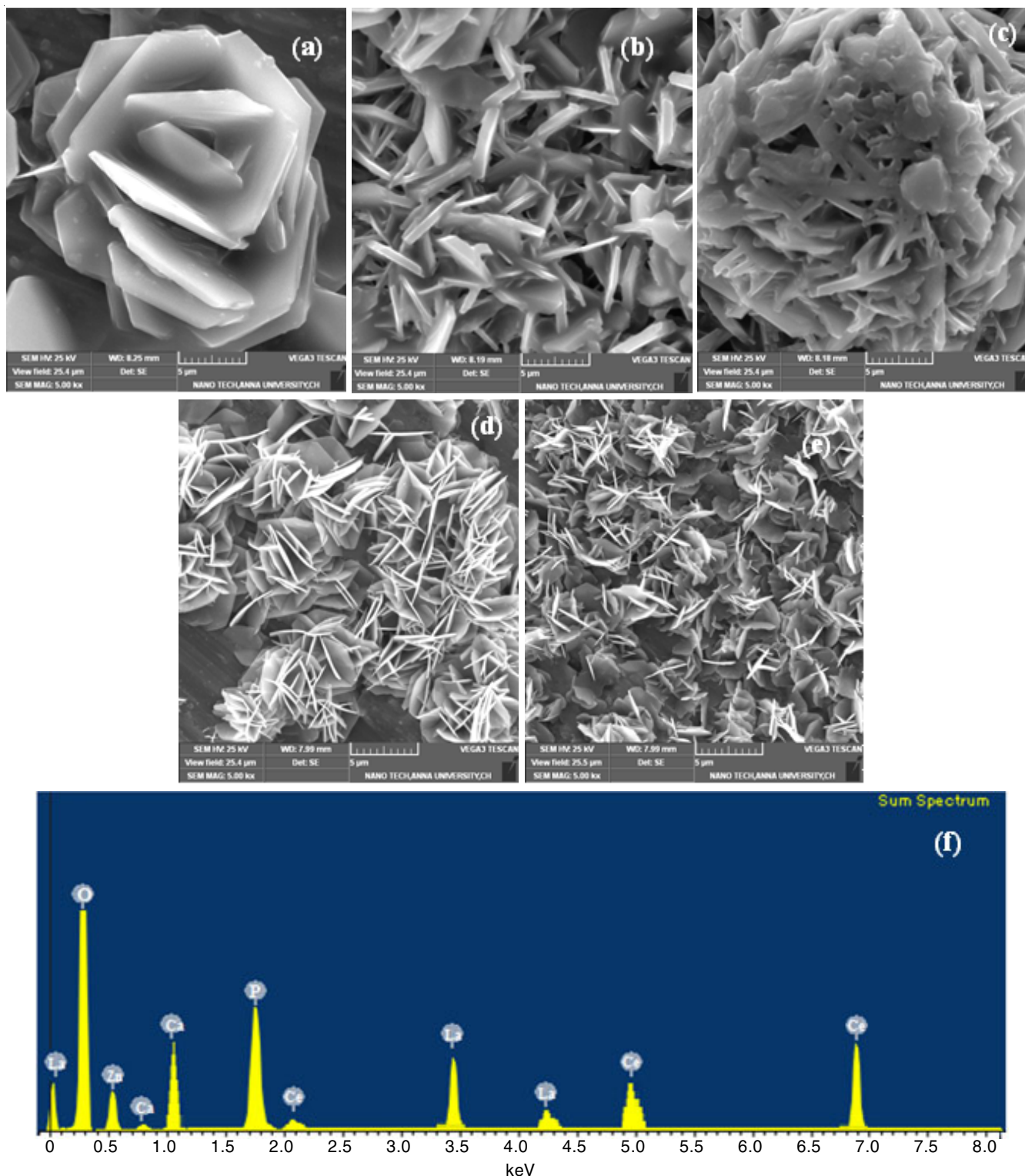


Fig. 3. SEM micrographs of (a) ZnO coating on different concentrations of 0.05 M (b) 0.1 M (c) 0.2 M (d) Ce, La- HAP coating (e) ZnO/Ce, La-HAP bilayer coating at 9 mA/cm² (f) EDAX spectrum of ZnO/Ce, La-HAP bilayer coating

are shown in Fig. 3a-c. The surface morphology of ZnO coatings in 0.05 M and 0.2 M concentrations consisted of flake like structure (Fig. 3a and 3c), which also showed that the surface structure was not uniform and some breakages. Moreover, the HRSEM images ZnO coatings of 0.1 M concentration of fully covered with flake like structure and was fixed as optimum.

Figs. 3d and 3e show the morphology of Ce,La-HAP coating on ZnO coated 316L SS (Fig. 3e) and on bare 316L SS (Fig.

3d). Both surface morphologies were flakes interconnected to microflower structure. The flakes interconnected structure permit the osteocompatibility and enhancement of cells and organs. Fig. 3f displays the energy dispersive X-ray analysis of ZnO/Ce, La-HAP coated on 316L SS. The EDAX spectrum indicates the presence of Ca, O, Zn, P, La and Ce ions, which supports the ZnO/Ce, La-HAP coating on 316L SS.

Electrochemical characterization

Potentiodynamic polarization studies: Anti-corrosion performance of the HAP overcome the problems of clinical applications of 316L SS. The corrosion resistance behaviour of uncoated, HAP coated, ZnO coated and ZnO/Ce,La-HAP coated 316L SS was explored in Ringers solution for long-term biomedical applications. Fig. 4a indicated the potentiodynamic polarization spectra of uncoated (I), HAP coated (II), ZnO coated (III) and ZnO/Ce,La-HAP (IV) coated on 316L SS in Ringers solution. As indicated from electrochemical values of potentiodynamic polarization parameters such as corrosion potential (E_{corr}), breakdown potential (E_b) and repassivation potential (E_{pp}) for the bare 316L SS (I) specimen were founded to be -865, +447 and -88 mV *versus* SCE, respectively. For HAP coated (II) 316L SS samples displayed E_{corr} , E_b , E_{pp} such as -790, +502 and 185 mV *versus* SCE, respectively. The electrochemical parameters of ZnO coated (III) 316L SS showed E_{corr} , E_b , E_{pp} such as -657, +628 and 258 mV *vs.* SCE, respectively.

The potentiodynamic polarization parameters of ZnO/Ce,La-HAP coated (IV) 316L SS demonstrated E_{corr} , E_b , E_{pp} values of -602, +790 and 320 mV *versus* SCE, respectively. Thus, the potentiodynamic polarization parameters of ZnO/Ce,La-HAP (IV) coated 316L SS were found to be positive direction shift when compared to uncoated (I), HAP coated (II), ZnO coated (III) on 316L SS. In specifically, ZnO/Ce,La-HAP (IV) coated 316L SS specimen possessed greater anticorrosion behaviour in Ringers solutions.

Electrochemical impedance spectroscopy studies (EIS): Electrochemical impedance spectroscopy studies (EIS) provide information about corrosion resistance in all coated 316L SS specimens in the Ringers solution. The nyquist curves achieved for the uncoated (I), HAP coated (II), ZnO coated (III) and ZnO/Ce,La-HAP (IV) coated 316L SS in Ringers solution are indicated in Fig. 4b. For uncoated (I) 316L SS polarization resistance (R_p) value show to be $1806 \Omega \text{ cm}^2$, respectively. The HAP coated (II) and ZnO coated (III) on 316L SS polarization resistance (R_p) values found to be 796 and 1543Ω

cm^2 . The (R_p) value obtained for ZnO/Ce,La-HAP (IV) coated on 316L SS substrate found to be $2136 \Omega \text{ cm}^2$ which was higher than uncoated, HAP coated and ZnO coated 316L SS. From these concluded electrochemical spectroscopy results ZnO/Ce,La-HAP coating on 316L SS is excellent corrosion protection in Ringers solution.

Antibacterial activity: The antibacterial movement of ZnO/Ce,La-HAP coating at five different concentrations was measured against the two pathogenic bacterial strains *E. coli* and *S. aureus* by the disc diffusion method. The antibacterial activity measured from zone of inhibition around ZnO/Ce,La-HAP coated samples at different volumes such as 25, 50, 75, 100 and 125 mL against *E. coli* and *S. aureus* is displayed in Fig. 5, which clearly indicated that ZnO/Ce,La-HAP coated samples displayed better antibacterial activity. Moreover, antibacterial activity against *E. coli* was higher than that against *S. aureus*, possibly due to the variation in cell walls between Gram-positive bacteria and Gram-negative bacterial strains. Generally, it was well achieved that cerium ion revealed to greater antibacterial activity. In this experimental work, asterisk symbol (*) represents a significant variance compared to control ($P < 0.05$), which indicated that the results are more significance compared than control.

Cell viability analysis and live/dead analysis with MC3T3-E1 cell lines: The cell proliferation of MC3T3-E1 cell lines on ZnO/Ce,La-HAP coating on 316L SS was evaluated using MTT analysis for 1 day, 3 days, 5 days and 7 days culture. After 1 day incubation, MTT mixture was additional incubated for 4 h at 37°C in a humidified 5% CO_2 atm. The quantity of proliferation cells increased as the increased time also increases (Fig. 6). The proliferation cells on excellent viability of 7 day's culture medium compare then 5, 3 and 1 days. As a result concluded on the increased viable cells of better osteocompatibility, without toxic effect and cell growth. Thus ZnO/Ce,La-HAP coating on 316L SS developed for biomedical applications.

Live/dead assay: The live/dead cells staining optically focused the MC3T3-E1 cells through fluorescence microscopy

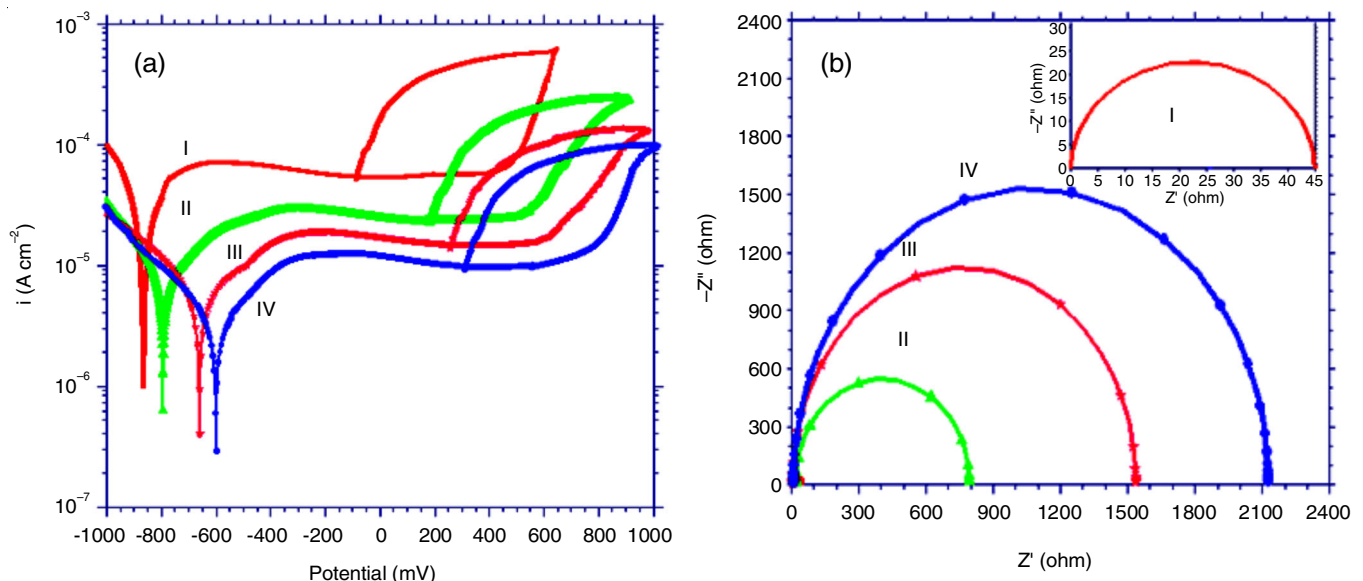


Fig. 4. (a) Potentiodynamic polarization curves (b) Impedance spectra of uncoated (I), HAP coated (II), ZnO coated (III), ZnO/Ce,La-HAP (IV) coated on 316L SS

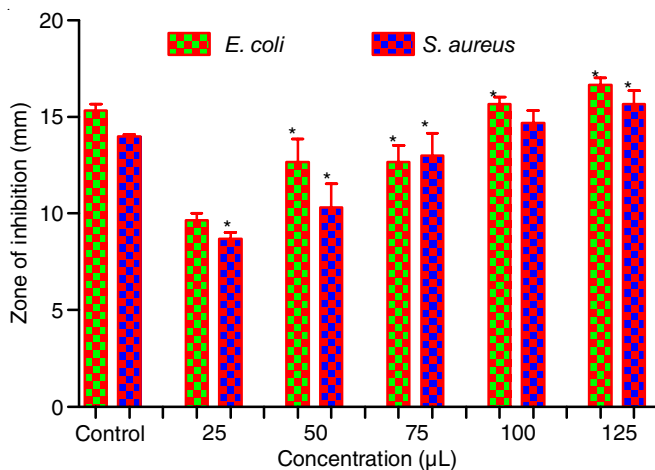


Fig. 5. Comparison of antibacterial activities of ZnO/Ce,La-HAP coating at various concentrations against pathogenic bacteria *E.coli* and *S. aureus*. (*) denotes a significant difference compare to the control ($P \leq 0.05$)

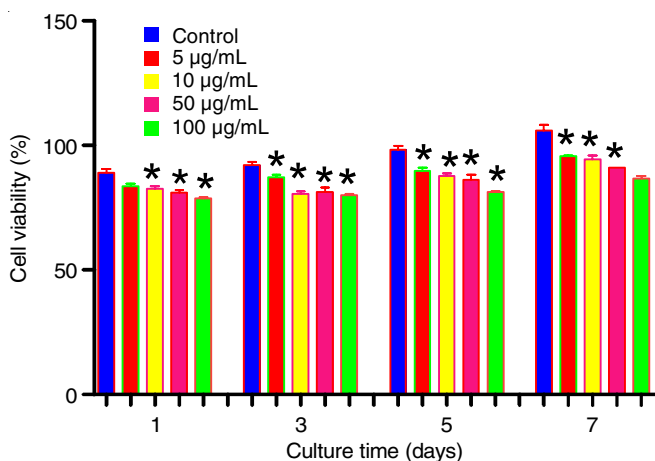


Fig. 6. *in vitro* Cell viability results of ZnO/Ce,La-HAP coating on MC3T3-E1 cells for 1,3,5 and 7 days. (*) denotes a significant difference compare to the control ($P \leq 0.05$)

achieved on ZnO/Ce,La-HAP coated 316L SS samples. The fluorescence microscopy of live/dead staining cultured on 3, 5 and 7 days. The live/dead microscopic images demonstrating the green were live cells and red were dead cells and used dye materials such as AM was used for green colour and ethidium

homodimer was used for red colour. Fig. 7a-b shows ZnO/Ce,La-HAP coated 316L SS samples after 3 and 5 days incubation period. Fig. 7b (5 days) showed that few cells were dead (red cells) and growth elongated morphology (green cells) as compared to Fig. 7a (3 days). Similarly, an increased in the incubation period and live cells also increases. Moreover, ZnO/Ce,La-HAP coated 316L SS samples indicated better number of live cells with good attachment after 7 days (Fig. 7c), when compared to the live/dead cells on 5 days (Fig. 7b) and 3 days (Fig. 7a). The fluorescent microscopic images clearly evidenced on the cell growth and spreading and good elongated morphology. Thus, ZnO/Ce,La-HAP coating can be served as an implant material in biomedical applications.

Conclusion

The present work revealed the enhancement of ZnO/Ce,La-HAP coating on 316L SS, which can meet the necessities of multi-functional medicinal activities (biocompatibility, antibacterial activity and osteocompatibility). The compositional evaluation and phase purity analysis using FT-IR and XRD spectra confirmed the formation of ZnO/Ce,La-HAP coating on 316L SS. The surface morphological evaluation (HRSEM) of ZnO/Ce,La-HAP coated on 316L SS exhibited the formation of flakes interconnected microflower structure, which results in the osteocompatibility and enhancement of cells and organs. Anti-corrosion performance of observed using by potentiodynamic polarization and electrochemical impedance spectroscopy (EIS) studies and found that ZnO/Ce,La-HAP coated on 316L SS samples significantly improved the corrosion resistance in Ringers solution. Moreover, this material also exhibited better antibacterial activity against *S. aureus* and *E. coli*. Finally, *in vitro* cell viability and fluorescent microscopic results showed that ZnO/Ce,La-HAP coating exhibits better cell growth, elongated morphology, non-toxic and cell viability of MC3T3-E1 cultures. Hence, ZnO/Ce,La-HAP bilayer coated samples will serve as a biomedical applications.

CONFLICT OF INTEREST

The authors declare that there is no conflict of interests regarding the publication of this article.

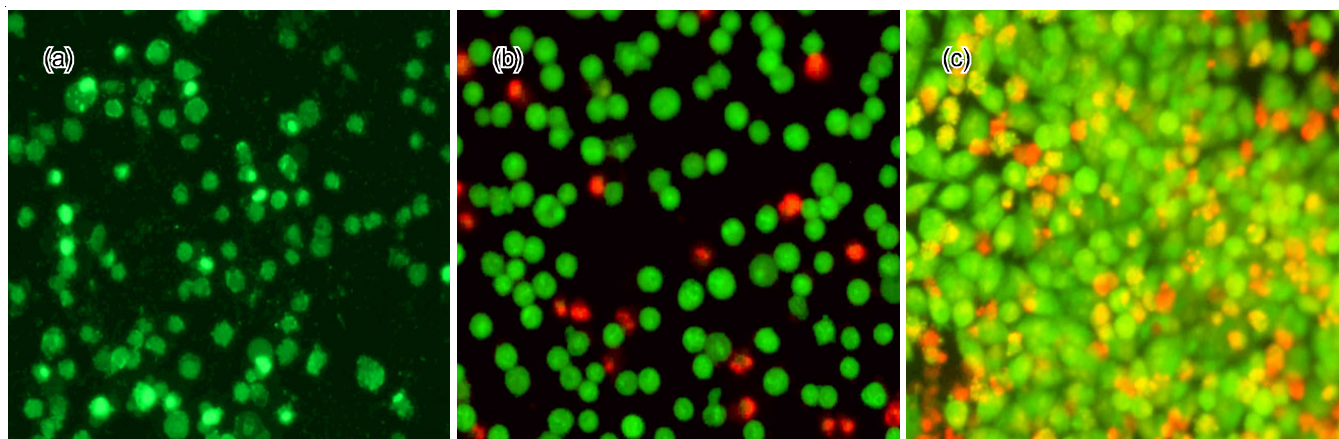


Fig. 7. Live /dead fluorescence microscopic images of (a) ZnO/Ce,La-HAP coating on 3 days (b) ZnO/Ce,La-HAP coating on 5 days (c) ZnO/Ce,La-HAP coating on 7 days

REFERENCES

1. F.G. Correa, J.V. Granados, M.J. Reyes and L. A. Q. Granados, *J. Chem.*, **2013**, 751696 (2013);
<https://doi.org/10.1155/2013/751696>
2. A.G. Mikos, S.W. Herring, P. Ochareon, J. Elisseeff, H.H. Lu, R. Kandel, F.J. Schoen, M. Toner, D. Mooney, A. Atala, M.E.V. Dyke, D. Kaplan and G. Vunjak-Novakovic, *Tissue Eng.*, **12**, 3307 (2006);
<https://doi.org/10.1089/ten.2006.12.3307>
3. L.C. Lucas, L.J. Bearden and J.E. Lemons, eds.: A.C. Fraker and C.D. Griffin, Second Symposium, American Society for Testing and Materials (ASTM), West Conshohocken, PA, pp. 208 (1985).
4. Y. Tang, S. Katsuma, S. Fujimoto and S. Hiromoto, *Acta Biomater.*, **2**, 709 (2006);
<https://doi.org/10.1016/j.actbio.2006.06.003>
5. T. Tuken, *Surf. Coat. Technol.*, **200**, 4713 (2006);
<https://doi.org/10.1016/j.surfcoat.2005.04.011>
6. E. De Las Heras, D.A. Egidi, P. Corengia, D. González-Santamaría, A. García-Luis, M. Brizuela, G.A. López and M.F. Martínez, *Surf. Coat. Technol.*, **202**, 2945 (2008);
<https://doi.org/10.1016/j.surfcoat.2007.10.037>
7. Y. Okazaki, E. Gotoh, T. Manabe and K. Kobayashi, *Biomaterials*, **25**, 5913 (2004);
<https://doi.org/10.1016/j.biomaterials.2004.01.064>
8. M.K. Lei and X.M. Zhu, *Biomaterials*, **22**, 641 (2001);
[https://doi.org/10.1016/S0142-9612\(00\)00226-X](https://doi.org/10.1016/S0142-9612(00)00226-X)
9. D.G. Wang, C.Z. Chen, J. Ma and G. Zhang, *Colloids Surf. B Biointerfaces*, **66**, 155 (2008);
<https://doi.org/10.1016/j.colsurfb.2008.06.003>
10. F. Bir, H. Khireddine, A. Touati, D. Sidane, S. Yala and H. Oudadesse, *Appl. Surf. Sci.*, **258**, 7021 (2012);
<https://doi.org/10.1016/j.apsusc.2012.03.158>
11. M. Chozhanathmisra, D. Govindaraj, P. Karthikeyan, K. Pandian, L. Mitu and R. Rajavel, *J. Chem.*, **2018**, 9813827 (2018);
<https://doi.org/10.1155/2018/9813827>
12. Y.W. Song, D.Y. Shan and E.H. Han, *Mater. Lett.*, **62**, 3276 (2008);
<https://doi.org/10.1016/j.matlet.2008.02.048>
13. Y. Han, T. Fu, J. Lu and K.W. Xu, *J. Biomed. Mater. Res.*, **54**, 96 (2001);
[https://doi.org/10.1002/1097-4636\(200101\)54:1<96::AID-JBM11>3.0.CO;2-U](https://doi.org/10.1002/1097-4636(200101)54:1<96::AID-JBM11>3.0.CO;2-U)
14. D.Y. Lin and X.X. Wang, *Ceram. Int.*, **37**, 403 (2011);
<https://doi.org/10.1016/j.ceramint.2010.08.018>
15. V. Stanic, S. Dimitrijevic, J. Antic-Stankovic, M. Mitriac, B. Jokic, I.B. Plešaš and S. Raičević, *Appl. Surf. Sci.*, **256**, 6083 (2010);
<https://doi.org/10.1016/j.apsusc.2010.03.124>
16. K.L. Wong, C.T. Wong, W.C. Liu, H.B. Pan, M.K. Fong, W.M. Lam, W.L. Cheung, W.M. Tang, K.Y. Chiu, K.D.K. Luk and W.W. Lu, *Biomaterials*, **30**, 3810 (2009);
<https://doi.org/10.1016/j.biomaterials.2009.04.016>
17. R.V. Suganthi, K. Elayaraja, M.I.A. Joshy, V.S. Chandra, E.K. Girija and S.N. Kalkura, *Mater. Sci. Eng. C*, **31**, 593 (2011);
<https://doi.org/10.1016/j.msec.2010.11.025>
18. C. Sridevi, S. Sathishkumar, S. Elavarasan, R. Rajavel and P. Maheswaran, *Chem. Sci. Trans.*, **7**, 319 (2018);
<https://doi.org/10.7598/cst2018.1483>
19. D.S. Morais, J. Coelho, M.P. Ferraz, P.S. Gomes, M.H. Fernandes, N.S. Hussain, J.D. Santos and M.A. Lopes, *J. Mater. Chem. B Mater. Biol. Med.*, **2**, 5872 (2014);
<https://doi.org/10.1039/C4TB00484A>
20. S. Majeed and S.A. Shivashankar, *J. Mater. Chem. B Mater. Biol. Med.*, **2**, 5585 (2014);
<https://doi.org/10.1039/C4TB00763H>
21. Y. Lin, Z. Yang and J. Cheng, *J. Rare Earths*, **25**, 452 (2007);
[https://doi.org/10.1016/S1002-0721\(07\)60455-4](https://doi.org/10.1016/S1002-0721(07)60455-4)
22. T. Naganuma and E. Traversa, *Biomaterials*, **35**, 4441 (2014);
<https://doi.org/10.1016/j.biomaterials.2014.01.074>
23. A. Tanaka, Y. Nishimura, T. Sakaki, A. Fujita and T. Shin-Ike, *J. Osaka Dent. Univ.*, **23**, 111 (1989).
24. T.J. Webster, E.A. Massa-Schlueter, J.L. Smith and E.B. Slamovich, *Biomaterials*, **25**, 2111 (2004);
<https://doi.org/10.1016/j.biomaterials.2003.09.001>
25. S. Shruti, F. Andreatta, E. Furlani, E. Marin, S. Maschio and L. Fedrizzi, *Appl. Surf. Sci.*, **378**, 216 (2016);
<https://doi.org/10.1016/j.apsusc.2016.03.209>
26. S.K. Dhoke, A.S. Khanna and T.J.M. Sinha, *Prog. Org. Coat.*, **64**, 371 (2009);
<https://doi.org/10.1016/j.porgcoat.2008.07.023>
27. C. Sridevi, S. Sathishkumar, P. Karthikeyan and P. Maheswaran, *Asian J. Chem.*, **31**, 1549 (2019);
<https://doi.org/10.14233/ajchem.2019.21967>
28. E. Kolanthai, V.S. Dikeshwar Colon, P.A. Sindu, V.S. Chandra, K.R. Karthikeyan, M.S. Babu, S.M. Sundaram, M. Palanichamy and S.N. Kalkura, *RSC Adv.*, **5**, 18301 (2015);
<https://doi.org/10.1039/C4RA14584D>